JACS
JOURNAL OF THE AMERICAN CHEMICAL SOCIETY
pubs.acs.org/JACS
Communication

Unconventional Route to High-Pressure and -Temperature Synthesis of GeSn Solid Solutions

George Serghiou,* Nicholas Odling, Hans Josef Reichmann, Kristina Spektor, Wilson A. Crichton, Gaston Garbarino, Mohamed Mezouar, and Anna Pakhomova

Cite This: J. Am. Chem. Soc. 2021, 143, 7920−7924
Read Online
ACCESS | Metrics & More | Article Recommendations | Supporting Information

ABSTRACT: Ge and Sn are unreactive at ambient conditions. Their significant promise for optoelectronic applications is thus largely confined to thin film investigations. We sought to remove barriers to reactivity here by accessing a unique pressure, 10 GPa, where the two elements can adopt the same crystal structure (tetragonal, $I4_1/amd$) and exhibit compatible atomic radii. The route to GeSn solid solution, however, even under these directed conditions, is different. Reaction upon heating at 10 GPa occurs between unlike crystal structures (Ge, $Fd\bar{3}m$ and Sn, $I4/mmm$), which also have highly incompatible atomic radii. They should not react, but they do. A reconstructive transformation of $I4/mmm$ into the $I4_1/amd$ solid solution then follows. The new tetragonal GeSn solid solution ($I4_1/amd$ a = 5.280(1) Å, c = 2.915(1) Å, Z = 4 at 9.9 GPa and 298 K) also constitutes the structural and electronic bridge between 4-fold and newly prepared 8-fold coordinated alloy cubic symmetries. Furthermore, using this high-pressure route, bulk cubic diamond-structured GeSn alloys can now be obtained at ambient pressure. The findings here remove confining conventional criteria on routes to synthesis. This opens innovative avenues to advanced materials development.

There is a strong long-standing drive to extend the functionality of (Si, Ge)-based technology from microelectronics into optoelectronics.[1] The indirect band gap of the cubic diamond-structured Si, Ge, and SiGe solid solutions makes this problematic.[2−4] A solid solution of Ge with Sn, however, can lead to direct band gap formation, which is thus being intensely investigated.[5−8] These investigations, however, are largely limited to thin films because Ge and Sn are unreactive at ambient pressure due to their dissimilar crystal and electronic structures and markedly different atomic radii.[9,10] Pressure, however, can have a profound effect on structural and electronic phase relations and therefore on reactivity,[11−13] leading also above 10 GPa to synthesis of a new cubic 8-fold coordinated GeSn solid solution.[14] At 10 GPa, a region of the phase diagram can be accessed where Ge and Sn may have the same crystal structure and favorable atomic radii ratios for solid solution formation.[11,15] We describe the endmember Ge and Sn phase relations here and investigate the special region where the intention is to have the two endmembers have the same crystal structure and compatible atomic radii. At between ambient and 10 GPa, Ge adopts the cubic $Fd\bar{3}m$ (c-Ge) structure, whereas Sn adopts a tetragonal $I4_1/amd$ structure (β-Sn, Strukturbericht Designation A5). At 10 GPa cubic Ge also transforms to the $I4_1/amd$ structure (β-Ge). Sn, on other hand, transforms above 10 GPa to another tetragonal phase with the $I4/mmm$ space group (t-Sn).[16] The only pressure where Ge and Sn are compatible according to the Hume−Rothery criteria[17] is at 10 GPa. In particular, at 10 GPa Ge and Sn can uniquely adopt the same crystal structure, $I4_1/amd$, and have atomic radii that differ by 11%,[18] well below the Hume−Rothery 15%[17] tolerance threshold for solid solution formation.

To investigate this region for creating reactivity to make a bulk Ge−Sn alloy, we employed a multianvil large volume press coupled with requisite and detailed *in situ* angle dispersive monochromatic synchrotron X-ray diffraction measurements.[18] The starting mixture was a 60:40 at. % c-Ge and β-Sn mixture, which was then compressed to 9.9 GPa. At 9.9 GPa, however, conversion to β-Ge has not occurred. Upon heating, β-Ge also does not appear (Figure 1a,c, Figure S2). This phase transition is severely kinetically hindered. Sn at 9.9 GPa is in the β-Sn structure with only a weak t-Sn presence (Figure 1a,c, Figure S2). Upon heating, the presence of t-Sn becomes more notable at 327 K, accompanied by c-Ge. At 352 K t-Sn is the principal Sn phase present, and by 384 K any residual β-Sn has disappeared, with c-Ge being the only Ge phase present. The first noticeable signs of a surprising reaction between c-Ge and t-Sn occur above 384 K. In particular between 298 and 384 K the (110) diffraction peak of t-Sn (black arrow at 489 K) shifts as normal to lower angles, due to thermal expansion (Figure 1a,c, Figure S2). It does so by 0.009 degrees. Between 384 and 489 K, however, this peak unexpectedly shifts to higher angle by 0.006 degrees due to uptake of smaller Ge by t-Sn (Figure 1a,c, Figure S2). Between 489 and 532 K the (110) peak shifts to higher angle by a further 0.006 degrees. But above 489 K concomitant with the additional Ge uptake in t-Sn, diffraction peaks of β-GeSn

Received: April 9, 2021
Published: May 19, 2021

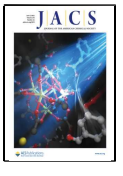

https://doi.org/10.1021/jacs.1c03765
J. Am. Chem. Soc. 2021, 143, 7920−7924

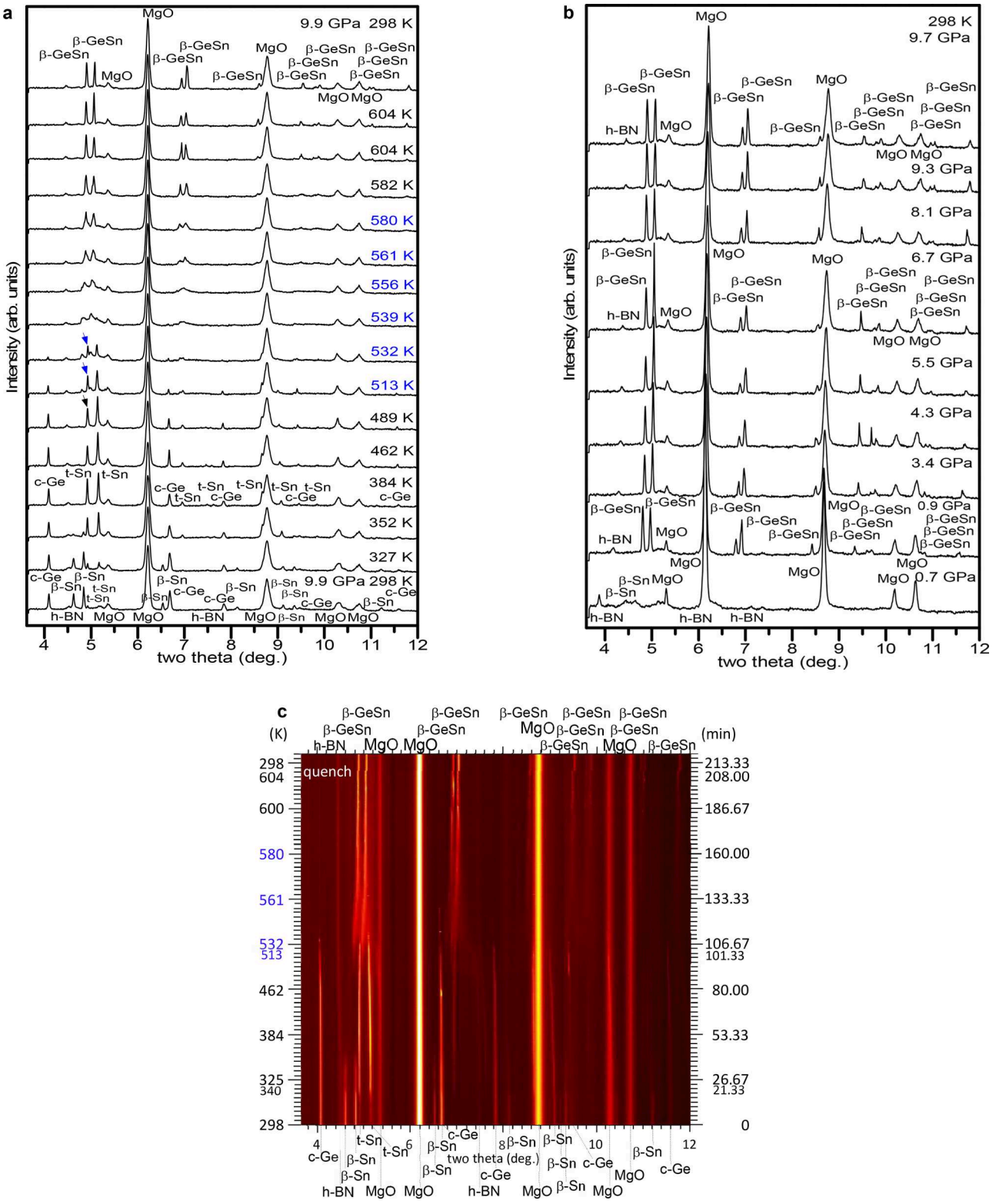

Figure 1. (a) Angle-dispersive X-ray diffraction patterns upon heating a c-Ge and t-Sn mixture (from a 60:40 starting mix) at 9.9 GPa in a multianvil device and formation of a β-GeSn solid solution upon heating {a = 5.294(1) Å, c = 2.926(1) Å at 9.9 GPa and 604 K (Figure S3 including Le Bail fitting)}.[18] A Vegard's law assessment[18] indicates a β-$Ge_{0.44}Sn_{0.56}$ composition upon temperature quenching {a = 5.280(1) Å, c = 2.915(1) Å at 9.9 GPa and 298 K (Figures S4 including Le Bail fitting)}.[18] Error assessments in pressure and temperature measurement are provided in the Supporting Information.[18] The Supporting Information[18] also includes a more detailed plot containing 31 diffraction patterns upon heating (Figure S2). The black arrow pinpoints the t-Sn diffraction peak ((110) plane) at a temperature where this peak is continuing to shift to higher angles (and hence Ge uptake is continuing) but before β-GeSn appears. The blue arrows in the ensuing two patterns (at 513 and 532 K) designate the continued shifting to the right of this peak and the concurrent emergence of β-GeSn solid solutions and the decline of the c-Ge and t-Sn patterns. The temperatures in blue designate the region throughout which the structural reconstruction (from $I4/mmm$ to $I4_1/amd$) and significant compositional changes occur in solid solution. The plot in the Supporting Information[18] shows this transitional region in much greater

https://doi.org/10.1021/jacs.1c03765
J. Am. Chem. Soc. 2021, 143, 7920−7924

Figure 1. continued

detail (Figure S2). (b) Patterns were collected on decompression. The solid solution is stable down to 0.9 GPa, with a broadened β-Sn pattern detected at 0.7 GPa (Figures S5−S12 including Le Bail whole pattern fittings are shown in the Supporting Information).[18] (c) Time−temperature−intensity−two theta plot at 9.9 GPa in the solid state and upon temperature quenching. The left horizontal bars are not scales, but references to correlate times on the right vertical axis with their corresponding temperatures on the left vertical axis. The blue-colored temperatures designate the region where the structural reconstruction (from $I4/mmm$ to $I4_1/amd$) and significant compositional changes occur in the new solid solution.

emerge and the $Fd\bar{3}m$ and $I4/mmm$ peaks decline in intensity. Between 556 and 604 K the only sample diffraction peaks present are those corresponding to the new β-GeSn solid solution, but they are broad and diffuse. This indicates structural disorder and compositional diversity, that is, a range of β-GeSn compositions. The peaks are also shifting to higher angles and gradually become more pronounced with temperature. This region hence indicates considerable restructuring as well as convergence on an overall higher Ge-containing β-GeSn phase. At 582 K the β-GeSn peaks are stronger and sharper and continue to gradually improve up to the highest annealing temperature of 604 K (Figure 1a, Figures S2 and S3). From 582 to 604 K, the β-GeSn peaks no longer significantly shift to higher angles. This is because a more limited shift to higher angles is compensated by a comparable shift to lower angles due to thermal expansion. The contribution of thermal expansion alone to β-GeSn peak shifting to lower angles is evident from the significant peak shifting to higher angles on temperature quenching (Figure 1a,c, Figures S2−S4). Using a Vegard's law estimation, the composition of the new tetragonal solid solution is β-$Ge_{0.44}Sn_{0.56}$ at 9.9 GPa and 298 K (Figure S4).[18] Since the β-solid solution has the same space group as β-Sn and unit cell parameters between those of the endmembers, it is reasonable to assume that all the atoms are on the high-symmetry Wyckoff 4a position. Upon decompression, the new tetragonal solid solution is retained down to 0.9 GPa (Figure 1b, Figures S5−S12). At 0.9 GPa a notable shoulder is also present on the left of the (011) peak (near 5 degrees), which is a harbinger of significant Sn ex-solution (Figure 1b). Accordingly, β-Sn peaks are observed on complete decompression accompanied by a nanocrystalline c-$Ge_{0.68}Sn_{0.32}$ pattern (Figure 2, Figure S13).[18] The nanocrystalline cubic diamond-structured crystallite size is evaluated to be about 7 nm.[18,19]

With the barriers to reactivity removed, allowing formation of the new tetragonal solid solution phase, we now consider the unusual route to its synthesis. We then describe how this new phase made possible by this unusual route plays a pivotal role in markedly expanding the group IVA materials' landscape.[14] According to the Hume−Rothery criteria, c-Ge and t-Sn are incompatible structurally and electronically for solid solution formation. They have unlike crystal structures, their atomic radii differ by a substantial 24%, well above the 15% tolerance ratio, c-Ge is an sp^3-hybridized semiconductor, whereas t-Sn is an sp-dehybridized metal[16−25] (Supporting Information).[18] With these characteristics, they should not react. But they do. Ge diffuses into the t-Sn structure, as seen by the shift to higher angles of the t-Sn(110) peak pinpointed by black and blue arrows (Figure 1a). This peak initially shifts to the left like the others (Figure 1a, Figure S2). Unlike the other peaks (and this one for pure t-Sn), which continue to shift to the left upon further heating, this one unexpectedly here then shifts to the right throughout the 384 to 532 K temperature regime (Figure 1a, Figure S2). Annealing and raising the temperature further cannot promote any additional

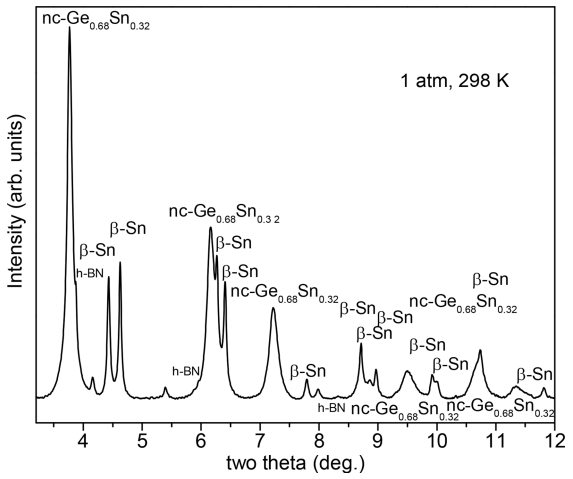

Figure 2. Nanocrystalline cubic diamond-structured phase with composition $Ge_{0.68}Sn_{0.32}$ based on a Vegard's law estimation,[18] together with β-Sn, is recovered upon complete release of pressure {$Fd\bar{3}m$, a = 5.925(1) Å, at 1 atm and 298 K, nanocrystalline size: 6.5 nm (Figure S13 including Le Bail whole pattern fitting)}.[18]

Ge incorporation into t-Sn. This now is not surprising, given the substantial Ge and Sn incompatibility, which causes strain in the t-Sn lattice with Ge incorporated. The strained t-$SnGe_x$ lattice however has an opportunity at 10 GPa. It can remove this strain and incorporate more of the surrounding abundant c-Ge ($Fd\bar{3}m$). It can do this by transforming from $I4/mmm$ to a favorable crystal structure, accessible for both elements at this specific pressure, $I4_1/amd$,[11,15,16] at the expense of the $Fd\bar{3}m$ and $I4/mmm$ phases. The $I4/mmm$ to $I4_1/amd$ transformation is however reconstructive.[24] This account is consistent with the evolution of the diffraction patterns (Figure 1a,c, Figure S2). Once the apparent limit is approached on Ge incorporation in t-Sn at 489 K, an $I4_1/amd$ broadened pattern with evolving peak shape profile emerges and gradually improves within a significant structural and compositional transition zone between 536 and 582 K (Figure 1a,c, Figure S2).[18] There is the additional question, however, of why would t-Sn accept any Ge to begin with, given their significant incompatibility with respect to the Hume−Rothery criteria? This may be traced back to the extremely favorable relative specific volume of β-GeSn with respect to t-Sn and c-Ge (Supporting Information).[18] In particular, from the specific volume point of view, there is no composition that would favor the reactants, t-Sn and c-Ge, over the product, β-GeSn. While this is not a sufficient criterion, it may provide a driving force for incorporation of enough Ge to trigger restructuring to the favorable $I4_1/amd$ phase. Notably this process would also hold true for β-Ge and t-Sn starting materials because their atomic radii ratios are also incompatible at 18%.[18] The new solid solution structure is stable upon temperature quenching and almost down to ambient pressure. At ambient pressure another significant transformation occurs to nanocrystalline diamond-structured nc-$Ge_{0.68}Sn_{0.32}$ together with β-Sn (Figure 2, Figure

https://doi.org/10.1021/jacs.1c03765
J. Am. Chem. Soc. 2021, 143, 7920−7924

S13). The Ge-rich cubic diamond-structured phase evidently results from ex-solution of β-Sn from the β-GeSn solid solution producing a Ge-richer composition, stable at ambient conditions in the nanocrystalline cubic diamond-structured phase.

These results are a fountainhead for developing new materials landscapes in the crystal chemically and technologically pivotal, from ceramic to semiconducting solid solution domain.[26,27] Here, the new β-GeSn phase, with its mixed covalent and metallic bonding and 6-fold coordination, is also the structural and electronic bridge between the 4-fold-coordinated cubic diamond-structured and new frontier 8-fold-coordinated body-centered cubic (bcc) Ge−Sn alloys.[14] With creation of this bridge, synthesis of the new bcc alloys is no longer, because of the incompatibility of Ge and Sn, limited to multiphase Ge and Sn starting mixtures. Now β-GeSn alloys will be used as a single-phase synthetic vehicle for preparing 8-fold-coordinated cubic alloys. This will allow us to closely investigate cubic alloy composition as well as crystal quality and stability formed from a known single-phase starting composition, as compared to synthesis from endmember physical mixtures.

The β-GeSn bridge is already a synthetic vehicle on its low-pressure side in making here bulk nanocrystalline cubic diamond-structured Ge−Sn, a hotly investigated system for optoelectronics, confined previously to thin films.[5−8] Through this work, investigation of bulk versus thin films can be examined together with the effect of crystal size and composition on direct band gap formation. Moreover, we are also pursuing high-pressure and -temperature synthesis of ternary (Ge−Sn−Si) systems. These can offer additional tunability[28] and entropic stabilization.[29,30] Stabilization may be further enhanced by low-temperature decompression, leading to complete recovery of novel Ge-rich octahedrally coordinated alloys with intriguing electronic, optical, and structural properties.[31]

■ ASSOCIATED CONTENT

Supporting Information

The Supporting Information is available free of charge at https://pubs.acs.org/doi/10.1021/jacs.1c03765.

Experimental procedures, atomic radii calculations, specific volume and Vegard's law calculations, detailed β-GeSn formation patterns, Le Bail fits and crystallographic data of experimental diffraction patterns, further recovered Ge−Sn pattern, and structural schematics (PDF)

Accession Codes

CCDC 2078828−2078829 contain the supplementary crystallographic data for this paper. These data can be obtained free of charge via www.ccdc.cam.ac.uk/data_request/cif, or by emailing data_request@ccdc.cam.ac.uk, or by contacting The Cambridge Crystallographic Data Centre, 12 Union Road, Cambridge CB2 1EZ, UK; fax: +44 1223 336033.

■ AUTHOR INFORMATION

Corresponding Author

George Serghiou − *School of Engineering, University of Edinburgh, EH9 3FB Scotland, United Kingdom*; Email: george.serghiou@ed.ac.uk

Authors

Nicholas Odling − *School of Geosciences, The Grant Institute, University of Edinburgh, Edinburgh EH9 3JW, U.K.*

Hans Josef Reichmann − *Deutsches GeoForschungsZentrum GFZ Telegrafenberg, 14473 Potsdam, Germany*

Kristina Spektor − *ESRF The European Synchrotron, 38000 Grenoble, France*

Wilson A. Crichton − *ESRF The European Synchrotron, 38000 Grenoble, France*

Gaston Garbarino − *ESRF The European Synchrotron, 38000 Grenoble, France*

Mohamed Mezouar − *ESRF The European Synchrotron, 38000 Grenoble, France*

Anna Pakhomova − *Deutsches Elektronen-Synchrotron (DESY), 22607 Hamburg, Germany*

Complete contact information is available at: https://pubs.acs.org/10.1021/jacs.1c03765

Notes

The authors declare no competing financial interest.

■ ACKNOWLEDGMENTS

Parts of this research were carried out at ID06 and ID27 at the European Synchrotron Radiation Facility (ESRF) in the context of CH5596 and CH5448. Parts of this research were also carried out at P02.2/PETRA at the German Electron Synchrotron (DESY), a member of the Helmholtz Association (HGF) in the context of DESY-D-I-20160758. We gratefully thank both institutions for their support. We also thank Mike Hall, Fraser Christensen, Euan Flett, Reik Suenkel, and Andreas Ebert for contributing to component micromanufacture, assembly, and characterization and Laurence Nigay for incisive comments on the manuscript.

■ REFERENCES

(1) Schilz, J.; Romanenko, V. N. Bulk growth of silicon-germanium solid solutions. *J. Mater. Sci.: Mater. Electron.* **1995**, *6*, 265−279.

(2) Hybertsen, M. S.; Louie, S. G. Electron correlation in semiconductors and insulators - band-gaps and quasi-particle energies. *Phys. Rev. B: Condens. Matter Mater. Phys.* **1986**, *34*, 5390−5413.

(3) Braunstein, R.; Moore, A. R.; Herman, F. Intrinsic optical absorption in germanium-silicon alloys. *Phys. Rev.* **1958**, *109*, 695−710.

(4) Serghiou, G.; Ji, G.; Koch-Müller, M.; Odling, N.; Reichmann, H.-J.; Wright, J. P.; Johnson, P. Dense Si_xGe_{1-x} ($0 < x < 1$) Materials Landscape Using Extreme Conditions and Precession Electron Diffraction. *Inorg. Chem.* **2014**, *53*, 5656−5662.

(5) Wirths, S.; Geiger, R.; von den Driesch, N.; Mussler, G.; Stoica, T.; Mantl, S.; Ikonic, Z.; Luysberg, M.; Chiussi, S.; Hartmann, J. M.; Sigg, H.; Faist, J.; Buca, D.; Grutzmacher, D. Lasing in direct-bandgap GeSn alloy grown on Si. *Nat. Photonics* **2015**, *9*, 88−92.

(6) Homewood, K. P.; Lourenco, M. A. The rise of the GeSn laser. *Nat. Photonics* **2015**, *9*, 78−79.

(7) Biswas, S.; Doherty, J.; Saladukha, D.; Ramasse, Q.; Majumdar, D.; Upmanyu, M.; Singha, A.; Ochalski, T.; Morris, M. A.; Holmes, J. D. Non-equilibrium induction of tin in germanium: towards direct bandgap $Ge_{1-x}Sn_x$ nanowires. *Nat. Commun.* **2016**, *7*, 11405.

(8) Elbaz, A.; Buca, D.; von der Driesch, N.; Pantzas, K.; Patriarche, G.; Zerounian, N.; Herth, E.; Checoury, X.; Sauvage, S.; Sagnes, I.; Foti, A.; Ossikovski, R.; Hartmann, J. M.; Boeuf, F.; Ikonic, Z.; Boucaud, P.; Grutzmancher, D.; El Kurdi, M. Ultra-low-threshold continuous-wave and pulsed lasing in tensile-strained GeSn alloys. *Nat. Photonics* **2020**, *14*, 375−382.

(9) Senaratne, C. L.; Wallace, P. M.; Gallagher, J. D.; Sims, P. E.; Kouvetakis, J.; Menendez, J. Direct gap $Ge_{1-y}Sn_y$ alloys: Fabrication and design of mid-IR photodiodes. *J. Appl. Phys.* **2016**, *120*, 025701.
(10) Massalski, T. *Binary Alloy Phase Diagrams*, 2nd ed.; Massalski, T., Ed.; ASM: OH, 1990; Vol. 2.
(11) Guillaume, C.; Serghiou, G.; Thomson, A.; Morniroli, J. P.; Frost, D. J.; Odling, N.; Mezouar, M. Tuning between Mixing and Reactivity in the Ge-Sn System Using Pressure and Temperature. *J. Am. Chem. Soc.* **2009**, *131*, 7550−7551.
(12) Serghiou, G.; Guillaume, C. L.; Jeffree, C. E.; Thomson, A.; Frost, D. J.; Morniroli, J. P.; Odling, N. Imaging of mixing and reaction in group IV systems recovered from high pressures and temperatures. *High Pressure Res.* **2010**, *30*, 44−50.
(13) Guillaume, C. L.; Serghiou, G.; Thomson, A.; Morniroli, J. P.; Frost, D. J.; Odling, N.; Jeffree, C. E. Correlation between Structural and Semiconductor Metal Changes and Extreme Conditions Materials Chemistry in Ge-Sn. *Inorg. Chem.* **2010**, *49*, 8230−8236.
(14) Serghiou, G.; Reichmann, H. J.; Odling, N.; Spektor, K.; Pakhomova, A.; Crichton, W.; Konôpková, Z. An unexpected cubic symmetry in group IV alloys prepared using pressure and temperature. *Angew. Chem., Int. Ed.* **2021**, *60*, 9009−9014.
(15) Young, D. A. *Phase Diagrams of the Elements*, 1st ed.; University of California Press: Berkeley, CA, 1991.
(16) Mujica, A.; Rubio, A.; Munoz, A.; Needs, R. J. High pressure phases of group IV, III-V, and II-VI compounds. *Rev. Mod. Phys.* **2003**, *75*, 863−912.
(17) Hume-Rothery, W.; Smallman, R. E. *The Structure of Metals and Alloys*, 5th ed.; The Chaucer Press: London, 1969.
(18) Supporting Information.
(19) Wang, H.; Liu, J. F.; He, Y.; Wang, Y.; Chen, W.; Jiang, J. Z.; Staun Olsen, J. High-pressure structural behaviour of nanocrystalline Ge. *J. Phys.: Condens. Matter* **2007**, *19*, 1−10.
(20) Di Cicco, A.; Frasini, A. C.; Minicucci, M.; Principi, E.; Itie, J. P.; Munsch, P. High-pressure and high-temperature study of phase transitions in solid germanium. *Phys. Status Solidi B* **2003**, *240*, 19−28.
(21) Cavaleri, M. E.; Plymate, T. G.; Stout, J. H. A pressure volume temperature equation of state for Sn(beta) by energy dispersive X-ray diffraction in a heated diamond-anvil cell. *J. Phys. Chem. Solids* **1988**, *49*, 945−956.
(22) Plymate, T. G.; Stout, J. H.; Cavaleri, M. E. Pressure volume temperature behavior and heterogeneous equilibria of the non-quenchable body-centered tetragonal polymorph of metallic tin. *J. Phys. Chem. Solids* **1988**, *49*, 1339−1348.
(23) Salamat, A.; Briggs, R.; Bouvier, P.; Petitgirard, S.; Dewaele, A.; Cutler, M. E.; Cora, F.; Daisenberger, D.; Garbarino, G.; McMillan, P. F. High-pressure structural transformations of Sn up to 138 GPa: Angle-dispersive synchrotron x-ray diffraction study. *Phys. Rev. B: Condens. Matter Mater. Phys.* **2013**, *88*, 104104.
(24) Katzke, H.; Bismayer, U.; Toledano, P. Theory of the high pressure structural phase transitions in Si, Ge, Sn and Pb. *Phys. Rev. B: Condens. Matter Mater. Phys.* **2006**, *73*, 134105.
(25) Christensen, N. E.; Methfessel, M. Density-functional calculations of the structural properties of tin under pressure. *Phys. Rev. B: Condens. Matter Mater. Phys.* **1993**, *48*, 5797−5807.
(26) Fadaly, E. M. T.; Dijkstra, A.; Suckert, J. R.; Ziss, D.; van Tilburgh, M. A. J. A.; Marvin, J.; Mao, C. Y.; Ren, Y. Z.; van Lange, V. T.; Korzun, K.; Kolling, S.; Verheijen, M. A.; Busse, D.; Roedel, C.; Furthmueller, J.; Bechstedt, F.; Stangl, J.; Finley, J. J.; Botti, S.; Haverkort, J. E. M.; Bakkers, E. P. A. M. Direct-bandgap emission from hexagonal Ge and SiGe alloys. *Nature* **2020**, *580*, 205−209.
(27) Oses, C.; Toher, C.; Curtarolo, S. High-entropy ceramics. *Nature Reviews Materials* **2020**, *5*, 295−309.
(28) Xu, C.; Senaratne, C. L.; Kouvetakis, J.; Menendez, J. Compositional dependence of optical interband transition energies in GeSn and GeSiSn alloys. *Solid-State Electron.* **2015**, *110*, 76−82.
(29) Manzoor, A.; Pandey, S.; Chakraborty, D.; Phillpot, S. R.; Aidhy, D. S. Entropy contributions to phase stability in binary random solid solutions. *npj Computational Materials* **2018**, *47*, 1−10.
(30) Dragoe, N.; Berardan, D. Order emerging from disorder. *Science* **2019**, *366*, 573−574.
(31) Li, R.; Liu, J.; Popov, D.; Park, C.; Meng, Y.; Shen, G. Experimental observations of large changes in electron density distributions in t-Ge. *Phys. Rev. B: Condens. Matter Mater. Phys.* **2019**, *100*, 224106.

https://doi.org/10.1021/jacs.1c03765
J. Am. Chem. Soc. 2021, 143, 7920−7924